NTNU
Norwegian University of
Science and Technology

Analysis of prediction methods for environmental conditions at the Hywind site

Analyse av beregningsmetoder for miljø på
Hywind-lokasjonen

Marit Stokke

Master of Energy and Environmental Engineering
Submission date: June 2016
Supervisor: Lars Sætran, EPT

Norwegian University of Science and Technology
Department of Energy and Process Engineering

NTNU
Norwegian University
of Science and Technology

Department of Energy
and Process Engineering

EPT-M-2016-129

MASTER THESIS

for

Student
Marit Stokke

Spring 2016

Analysis of prediction methods for environmental conditions at the Hywind site

Analyse av beregningsmetoder for miljø på Hywind-lokasjonen

The economic benefits of understanding the role of the ocean in the climate system are enormous. And accumulating evidence of man-made climate change has brought these issues to the attention of the public. These concerns coincide with recent successes in long-term weather forecasting (associated with El Niño) and with advances that enable detailed measurement of climate variables. These factors imply that climate studies will be a significant path for future research in oceanography. The development of long-term forecasting skill raises challenging scientific problems. These include: understanding and quantifying turbulent mixing, convection, water-mass formation and destruction; the thermohaline circulation and its coupling to the wind-driven circulation; the generation, maintenance, and destruction of climatic anomalies; climatic oscillations and the coupling of the ocean and atmosphere on seasonal, decadal and interdecadal timescales; the physics of exchange processes between the ocean and the atmosphere. All these problems are of fundamental scientific and practical importance.

Modelling, analysis and prediction of environmental conditions are important for calculating environmental loads on structures. Some of the prediction methods are presented in DNV Recommended Practice DNV-RP-C205 "Environmental conditions and environmental loads". For this thesis work we have access to 2 years of environmental data from the Seawatch buoy at the Hywind site west of Karmøy. This data bank enables an opportunity to test and evaluate prediction methods for environmental conditions – methods that are presented in the reference above or can be found in the research literature.

Within 14 days of receiving the written text on the master thesis, the candidate shall submit a research plan for his project to the department.

When the thesis is evaluated, emphasis is put on processing of the results, and that they are presented in tabular and/or graphic form in a clear manner, and that they are analyzed carefully.

The thesis should be formulated as a research report with summary both in English and Norwegian, conclusion, literature references, table of contents etc. During the preparation of the text, the candidate should make an effort to produce a well-structured and easily readable report. In order to ease the evaluation of the thesis, it is important that the cross-references are correct. In the making of the report, strong emphasis should be placed on both a thorough discussion of the results and an orderly presentation.

The candidate is requested to initiate and keep close contact with his/her academic supervisor(s) throughout the working period. The candidate must follow the rules and regulations of NTNU as well as passive directions given by the Department of Energy and Process Engineering.

Risk assessment of the candidate's work shall be carried out according to the department's procedures. The risk assessment must be documented and included as part of the final report. Events related to the candidate's work adversely affecting the health, safety or security, must be documented and included as part of the final report. If the documentation on risk assessment represents a large number of pages, the full version is to be submitted electronically to the supervisor and an excerpt is included in the report.

Pursuant to “Regulations concerning the supplementary provisions to the technology study program/Master of Science” at NTNU §20, the Department reserves the permission to utilize all the results and data for teaching and research purposes as well as in future publications.

The final report is to be submitted digitally in DAIM. An executive summary of the thesis including title, student’s name, supervisor's name, year, department name, and NTNU's logo and name, shall be submitted to the department as a separate pdf file. Based on an agreement with the supervisor, the final report and other material and documents may be given to the supervisor in digital format.

☐ Work to be done in lab (Water power lab, Fluids engineering lab, Thermal engineering lab)
☐ Field work

Department of Energy and Process Engineering, 13. January 2016

Olav Bolland
Department Head

Lars Sætran
Academic Supervisor

Abstract

The increasing amount of offshore installations and maintenance are rising the importance of reliable weather forecast. To carry out an offshore operation it is necessary that the waves are not too high nor the wind and currents too strong. By providing good weather forecast, such conditions are avoided. If the forecast predicts worse weather, an offshore operation might be canceled unnecessarily, causing expensive losses.

In the process of building and testing the floating wind turbine, Hywind Demo, weather forecast models with higher resolutions than regularly was established. In addition, wind, waves and currents are well documented for the Hywind Demo site by a Seawatch buoy. By use of these data, an assessment of the quality of the weather forecast has been performed.

The comparison of the weather forecast one day ahead with the measured data, gave following results. The correlation for currents are low. For wind and waves, the correlation are relatively good. Statistically, does one year of weather forecast give a reasonable estimate of what to expect at the site. Exceptions are that stronger surface currents will most likely occur and lower waves are to be expected.

Samandrag

Det vert stadig gjennomført fleire offshore operasjonar, noko som aukar behovet for påliteleg vêrvarsel. For at ein operasjon skal gå trygt føre seg, er det viktig at bølgjene ikkje er for høge og at vinden og havstraumen ikkje er for sterk. Når vêrvarselet er godt, unngår ein slike situasjonar. Det er ei heller ønskjeleg at det varslast styggare vêr enn observert, då dette kan kanseller operasjonar unødig og føre til økonomiske tap.

Då den flytande vindturbin, Hywind Demo, skulle byggjast, vart det utvikla vêrmodellar med ekstra høg oppløysing. I tillegg, er vind, bølgjer og havstraum godt dokumentert av ei Seawatch bøye lokalisert like ved turbinen. Ved hjelp av desse data, har kvaliteten på vêrmeldinga vorte kartlagt.

Samanlikninga mellom varselet ein dag fram i tid og bøyemålingane, gav følgjande resultat. Korrelasjonen for havstraum er låg. Korrelasjonen for vind og bølgjer, er relativt god. Statistisk, vil eit år med vêrvarsel gi eit brukbart estimat av kva som kan forventast på staden. Unntaka er, at sterkare havstraum vil truleg førekome og lågare bølgjer kan forventast.

A comparison of short-term weather forecast with the measured conditions at the Hywind Demo site

Marit Stokke
Master thesis, June 2016
Department of Energy and Process Engineering
Norwegian University of Science and Technology

***Abstract*—The companies operating at the Hywind Demo site have experienced that the weather forecast fails, especially when considering the ocean current. This work has compared short-term weather forecast with measured data from a Seawatch buoy. It was obtained a low correlation for currents. For wind and waves the correlation were relatively good. Statistically, does one year of weather forecast give a reasonable estimate of what to expect at the site. Exceptions are that stronger surface currents will most likely occur and lower waves are to be expected.**

***Index terms*—Weather forecast, verification, buoy, offshore operation.**

I. Introduction

The increasing amount of offshore installations and maintenance are rising the importance of reliable weather forecast. To carry out an offshore operation it is necessary that the waves are not too high nor the wind and currents too strong. By providing good weather forecast, such conditions are avoided. If the forecast predicts worse weather, an offshore operation might be canceled unnecessarily, causing expensive losses.

In the process of building and testing the floating wind turbine, Hywind Demo [1], weather forecast models with higher resolutions than regularly was established. These models are still active and today an improved ocean current model has been implemented [2].

At the Hywind Demo site, the main flow direction of the wind is along the coastline [3]. To describe the energy of the waves at the location, a wave spectrum is applied. Waves are either induced by local wind or arriving from other areas [4]. To perform an offshore operation at the site, a significant wave height of 1.5 m is the upper, permissible limit.

The turbine is located south-west of Karmøy and along the Norwegian Coastal Current, which is mainly a composite of Baltic outflow and freshwater runoff from Norway [5]. The area is exposed to eddies causing extreme current speeds [6]. They are produced of sudden outbreaks of water from the Skagerrak [5].

Wind, waves and currents are well documented for the Hywind Demo site by a Seawatch buoy. By use of these data, an assessment of the quality of the weather forecast has been performed.

List of Abbreviations

ADCP	Acoustic Doppler current profiler
CD	Current direction
CS	Current speed
FAR	False alarm ratio
HR	Hit rate
POM	The Princeton Ocean Model
ROMS	The Regional Ocean Modeling System
SWAN	Simulating Waves Nearshore
WD	Wind direction
WS	Wind speed

II. Forecast methods

The weather forecast and the information about the models given later on have been provided by the Norwegian Meteorological Institute (MET Norway) [2]. The data available for this project, are short-term forecast models that have been run once a day for currents, while twice a day for wind and waves. All of the models predict the weather +1, +2, +3 etc. hours ahead. The forecast of wind and waves ends at +48, while the ocean current at +66. The first hours a model is running does not give a reliable result. It is common to assume that the models have stabilized after three hours.

In England, The European Centre for Medium-Range Weather Forecast (ECMWF) is located [7]. It is a cooperation between meteorological institutes, which provides all of them with information about long term (more than 3 days ahead) global atmospheric conditions.

A. Atmosphere model

The obtained atmospheric model is called UM1 and covers the Hywind area on a 1 km scale. Initially, it gets large scale information and boundary conditions from ECMWF. The model is run with 38 layers in the vertical and solves the Navier-Stokes equation. Among the parameters the model include, are radiation, atmospheric stability, humidity, terrain, temperature and the rotation of the earth.

B. Wave models

The Wave Model (WAM) solves the wave energy balance equation. By use of an implicit numerical scheme, the model Simulating Waves Nearshore (SWAN) is a cost efficient version of WAM. SWAN is used at this site. It includes shallow water effects as depth induced wave breaking and bottom friction. The model has a grid size of 500 m x 500 m. The wind by UM1 is used as a driving force and wave models with less resolution are used as boundary conditions.

C. Ocean models

The Princeton Ocean Model (POM) is an ocean model that contain driving forces as atmospheric fields, water inflow from rivers and inflow from the Baltic Sea [8]. MET Norway used a version of POM, called MI-POM, having a mesh size of 1.5 km.

The Regional Ocean Modeling System (ROMS) is a more sophisticated ocean model [9], developed for coastal shelf seas. A version of ROMS, NorKyst-800, is what is used today. The grid has a mesh size of 800 m. The model is based on basically the same forces as POM.

III. The Seawatch buoy

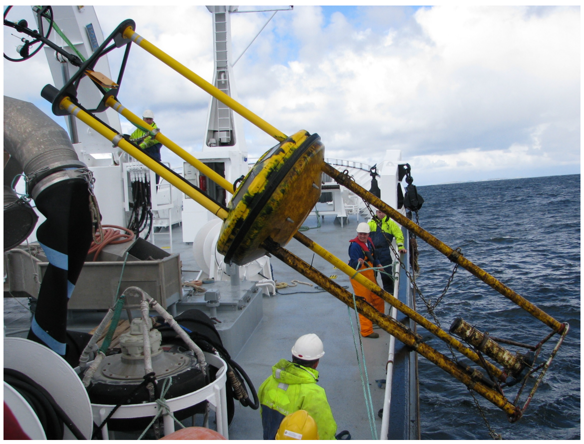

Fig. 1. The Seawatch buoy

In 2009, the Seawatch buoy [10] was installed 200 m west of Hywind Demo, positioned south-west of Karmøy. The specific location was 59°08.42'N, 5°01.78'E. Figure 1 is from one of the service operations performed on the buoy. In Figure 2 a description of the buoy and its instruments can be seen. The buoy was taken onshore in 2011 and the renovated version was redeployed January 19th 2016. The renovated buoy measures current at other depths than the old version. The following metocean parameters are measured by the sensors printed in italics.

- Wind speed, direction and gust at 3.5 m above the sea level. *Yound, 85106-19 Ultrasonic*
- Wave height, period and direction relative to mean sea level. *Seatex, MRU-4*
- Current speed and direction, from 3 to 180 m depth. *RDI, ADCP 150 kHz - Sentinel*
- Surface current speed and direction. *Nortek, Aquadopp*
- Air pressure at the sea level. *Vaisala, PTB 330 CLASS A*
- Water temperature at 2 and 3 m depth. *Seabird, SBE 37-SIP*
- Conductivity of the water at 2 m depth. It is used in combination with temperature to calculate the salinity. *Seabird, SBE 37-SIP*

The accuracy of the measurements of current speed are; "0.3% of the water velocity relative to ADCP ±0.3 cm/s" [11]; while it is "1% of measured value ±0.5 cm/s" [12] for the surface current speed. The accuracy of the wave height is "5 cm or 5% whichever is highest" [13] and the wind speed might have a deviation of "±2% or 0.1 m/s" [14].

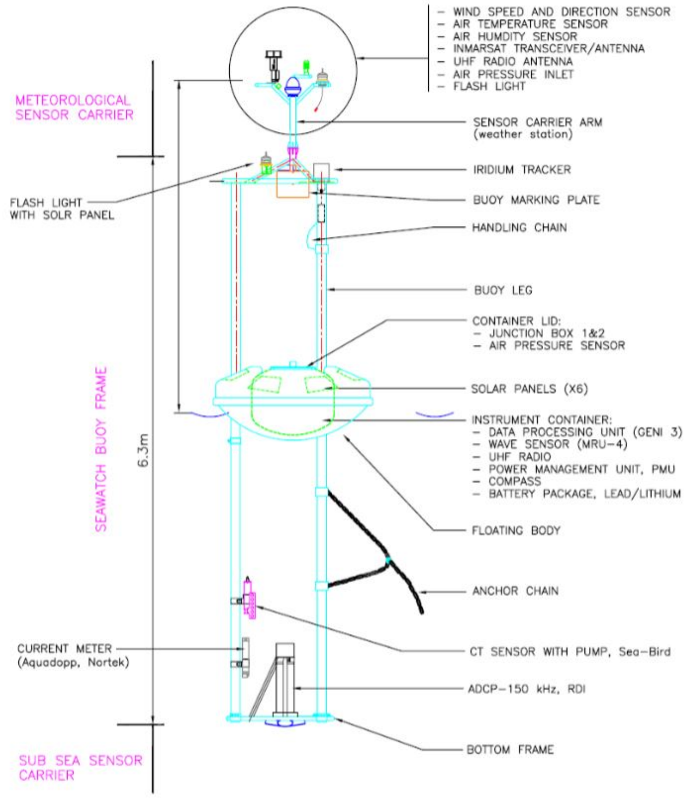

Fig. 2. Instrumentation on the Seawatch buoy

A. Wind

The buoy measurements of wind are done at H = 3.5 m above sea level, while the weather forecast is at 10 m. Therefore the measured wind speed, U(H), have been extrapolated by use of Equation 1, which assumes the wind to follow a power law profile [15].

$$U(z) = U(H)\left(\frac{z}{H}\right)^{\alpha} \tag{1}$$

z is the height of interest and α is the power coefficient sat to 0.11 according to Hsu et al. [16]. It is an ongoing discussion, which value of α that is the best. Another established method to extrapolate the wind speed is the logarithmic wind speed profile, which assumes neutral atmospheric conditions [15]. In this case no information is given about the atmospheric stability and the power law profile is therefore a more reliable choice. The wind direction of the weather forecast are compared to the wind direction measured at H, since no simple method exists to transfer measurements of wind direction at one height to another. The direction describes where the wind comes from.

B. Waves

To describe waves, it is common to apply a spectral wave model. It assumes that waves can be divided into two parts, wind sea and swell sea [4]. Wind sea is generated by wind at the site, while swells are waves entering from other areas. Wind sea has a low altitude and a high frequency and therefore contains a low amount of energy [17]. The Seawatch buoy defines wind sea as the waves with frequencies between 0.10-0.50 Hz. When a wave travels some distance, its height and energy increases, while the frequency decreases [17]. The Seawatch buoy defines swell as a wave with frequency between 0.04-0.10 Hz. Several factors are present in the formation of waves, but a significant amount of the energy transfer to the waves come from the wind [18].

Based on the buoys movement, heave, roll and pitch, a wave spectra is calculated. The wave spectrum at a location describes the energy of the waves passing. T_p, is the period of the spectral peak and corresponds to the wave period with the highest energy [4]. The significant wave height, H_{m0}, can be found from the 0th spectral momentum, m_0, as described by Equation 2 [17]. In the same way, the significant wave height of swells, H_{m0a}, are calculated from the momentum of the swell components of the wave spectra.

$$H_{m0} = 4\sqrt{m_0} \tag{2}$$

C. Ocean current

For the current, the direction tells where it flows towards. This section will mention some of the physical aspects of the ocean current at the site.

The Norwegian coastal current is known to be the main driving force of the current at the Hywind Demo site along with inertial oscillations [19]. After a period with strong wind, the wind speed decreases and then strong currents are observed, this is called inertial oscillations [19]. Coriolis force and gravity are important for the behaviour of the current [20]. The tidal differences are small at the location of Hywind Demo, as the mean difference between low and high tides is approximately 0.32 m [21].

The presence of eddies causing extreme current speeds was first confirmed in the 1970s [22] and the Hywind Demo area is exposed to eddies produced of sudden outbreaks of water from the Skagerrak [5], [6]. The fjord between Stavanger and Utsira is spacious, therefore the fjord mouth is highly exposed to internal waves, which are generated in the boundaries between two water masses of different density [5]. An internal wave causes no elevation of the sea surface, but the amplitude might be 30 m [5]. The associated currents may affect the flow of the ocean at the Hywind Demo site.

IV. Method for comparison of the weather forecast and the buoy measured parameters

A. Verification method

$$r = \frac{\sum_{i=1}^{n}(x_i - \bar{x})(y_i - \bar{y})}{\left[\sum_{i=1}^{n}(x_i - \bar{x})^2 \sum_{i=1}^{n}(y_i - \bar{y})^2\right]^{\frac{1}{2}}} \tag{3}$$

To verify the weather forecast the linear correlation coefficient, r, will be calculated by Equation 3 [23]. This is an estimate of the correlation coefficient, called the sample correlation coefficient [24]. r is the fraction between the covariance of observations and predictions, and the variance of observations times the variance of predictions. The covariance is a result of the joint probability distribution, while the variances are results of the marginal distributions [24], [25].

The marginal distribution of observations, gives information about how many times a certain case was observed, independent of what was predicted. The joint probability distribution of observations and predictions, gives the probability that a certain combination of observation and prediction occur, like a three dimensional scatter plot. From the joint probability distributions, different percentages will be calculated and presented.

The mean and standard deviation of the marginal distributions and the maximum and 99.9%-quantile will be listed for both observed and predicted parameters [24]. The 99.9%-quantile is the value that 99.9% of the data are below or equal to.

For a visual view, both scatter plots and quantile-quantile (q-q) plots will be made [24]. In this case, the q-q plot is a comparison of the marginal distributions of the observed data and of the predicted data, more specifically a plot of the points (x%-quantile$_{observed}$, x%-quantile$_{predicted}$), x is from 0 to 100%. The q-q plot tells how well the ordered data correlate, while the scatter plot compares the values at the same time. If the weather forecast is perfect, both plots show a straight line, e.q. the observed value is equal to the predicted and the marginal distributions are similar. If the weather forecast follows the same distribution as the observed result, but the values of the abscissas are different, the slope of the straight line in the q-q plot will be a result of this difference. For this particular case, the weather forecast and the measurements are from the same period and ideally the probability distributions will have the same shape and size, giving a q-q plot with a slope of 1.

Multiple variables exist to describe the quality of weather forecast, a selection will be presented in this paper. The hit rate, HR, is the fraction between the number of times an event was both predicted and observed, and the total times the event was observed [26]. HR has a optimal score of 1 and the total range is from 0 to 1. The false alarm ratio, FAR, is the fraction between the number of times a predicted event was not observed and the total number of times it was predicted [26]. FAR has an optimal and minimum score of 0 and a maximum value of 1. As the difference between the two ocean models are of special interest, the results of HR and FAR for different events will be presented together.

B. The period 2009-2011

The following parameters were available for both the weather forecast and the buoy measured parameters.

- Significant wave height
- Significant wave height of swells

- Period of spectral peak
- Wind speed and direction
- Mean Sea Level Pressure
- Current speed and direction
- Salinity

Data of wind and waves are available from October 2009 to August 2011. Twelve hours will be used from each run of the models. The ocean current data are provided for October 2009 to December 2010, and 24 hours will be used from each run of the models. In the plots, the forecast +24 is the first hour used for comparison with the buoy measurements. When a parameter is marked with, e.g. +24, 24 is the first hour used from the run of the model.

The buoy measurements of wind will be compared to the forecast at 10 m. The ocean model POM are compared to measurements and plotted for currents at 10 m and 100 m depth. It has been assumed that the current at 10 m depth for POM can be compared to the surface current for ROMS.

The atmospheric forecast is valid the actual hour, while the forecast for waves and currents are mean values for that hour. At the Seawatch buoy, measurements are sampled at 1 Hz and saved as 10 minute mean values. Therefore, the forecast of wind are compared to 10 minute mean observed data, while the forecast of waves and currents are compared to the average of one hour ($\pm$ 30 minute interval). To compute the mean current direction, the Matlab function by Berens [27] have been used, as it allows for 0° and 360° to be the same point [28], [29].

C. Ocean current data from 2016

The available period of both forecast and buoy measurements are January 19th to February 14th. This year MET Norway uses the improved ocean model ROMS and from each run of the model the provided forecast ends at +24. In this period, the measured data are saved as 20 minute mean values, hence the forecast for each hour will be compared to the mean of three 20 minute mean values. As this comparison period is one month, the 99.9%-quantile is equal to the maximum and the 99%-quantile will be listed instead. The current at 100 m depth and at the surfcae will be investigated. The surface current is roughly based on the volume between 1 m depth and the surface.

V. Result

A. The period 2009-2011

The different correlation coefficients are listed in Table II. Values of standard deviation and mean are listed in Table III, with maximum and 99.9%-quantile values in Table IV. Information about the data recovery rate and the number of comparison points are listed in Table I.

TABLE I
THE TOTAL NUMBER OF POINTS COMPARED AND THE LENGTH OF THE COMPARISON PERIOD AND ITS DATA RECOVERY RATE.

Parameter	Length of period	Number of points	Data recovery rate
Wind	1 year 10 months	10601	74%
Waves	1 year 10 months	12195	76%
Current 10m	1 year 1 month	7631	90%
Current 100m	1 year 1 month	7682	91%
Pressure	1 year 10 months	10617	75%
Salinity	1 year 1 month	1026	71%

TABLE II
THE CORRELATION COEFFICIENTS BETWEEN THE WEATHER FORECAST +3/+24/+48 AND THE MEASURED VALUES.

Parameter	r_{+3}	r_{+24}	r_{+43}
Wind speed 10 m	0.88	0.82	
Wind direction 10 m	0.75	0.70	
Pressure	1.00	1.00	
Significant wave height	0.94	0.92	
Significant wave height of swells	0.91	0.91	
Period of spectral peak	0.70	0.67	
Current speed 10 m	0.34	0.34	0.35
Current direction 10 m	0.18	0.16	0.16
Current speed 100 m	0.24	0.24	0.25
Current direction 100 m	0.21	0.17	0.17
Salinity	0.18	-0.13	-0.16

TABLE III
VALUES OF MEAN AND STANDARD DEVIATION.

	Mean		Standard deviation	
	Predicted	Observed	Predicted	Observed
$WS10m_{+24}$ [m/s]	7.41	7.35	3.59	3.62
$H_{m0,+3}$ [m]	1.83	1.56	1.08	0.90
$H_{m0,+24}$ [m]	1.83	1.56	1.07	0.90
$H_{m0a,+24}$ [m]	0.65	0.58	0.72	0.63
$T_p, +3$ [s]	8.39	8.37	2.48	2.30
$T_p, +24$ [s]	8.33	8.37	2.51	2.30
$CS10m_{+3}$ [m/s]	0.28	0.31	0.18	0.18
$CS10m_{+24}$ [m/s]	0.28	0.31	0.18	0.18
$CS100m_{+3}$ [m/s]	0.15	0.16	0.12	0.09
$CS100m_{+24}$ [m/s]	0.15	0.16	0.11	0.09

TABLE IV
VALUES OF 99.9%-QUANTILE AND MAXIMUM.

	99.9%-quantile		Max	
	Predicted	Observed	Predicted	Observed
$WS10m_{+24}$ [m/s]	19.33	18.08	20.96	19.80
$H_{m0,+3}$ [m]	7.71	6.65	9.03	8.16
$H_{m0,+24}$ [m]	7.10	6.65	9.10	8.16
$H_{m0a,+24}$ [m]	5.13	5.36	7.17	7.10
$T_p, +3$ [s]	17.82	16.14	17.82	18.38
$T_p, +24$ [s]	17.82	16.14	17.82	18.38
$CS10m_{+3}$ [m/s]	0.93	1.11	1.03	1.18
$CS10m_{+24}$ [m/s]	1.00	1.11	1.15	1.18
$CS100m_{+3}$ [m/s]	0.65	0.59	0.73	0.71
$CS100m_{+24}$ [m/s]	0.66	0.59	0.71	0.71

In Figures 3-11 are the scatter plot grey dots, the q-q plot blue dots and the red line shows the observation equal to the forecast.

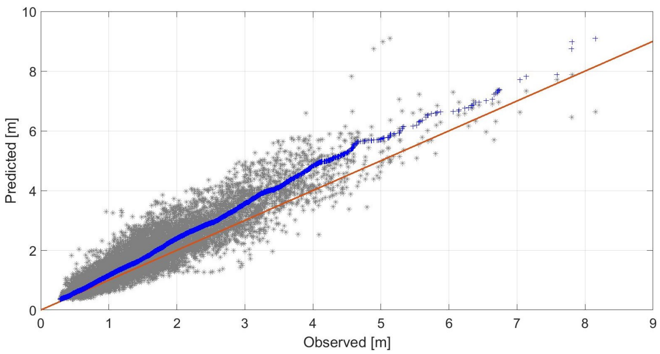

Fig. 3. The significant wave height, forecast +24 (SWAN).

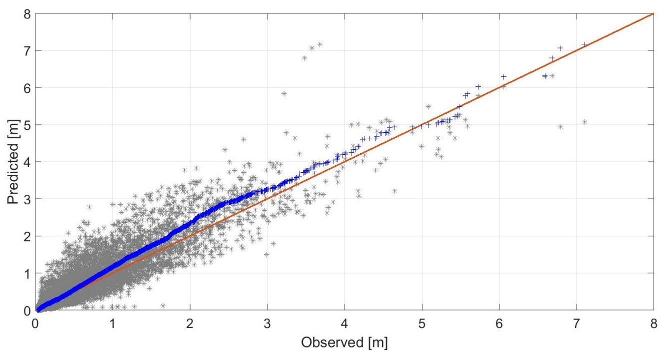

Fig. 4. The significant wave height of swells, forecast +24 (SWAN).

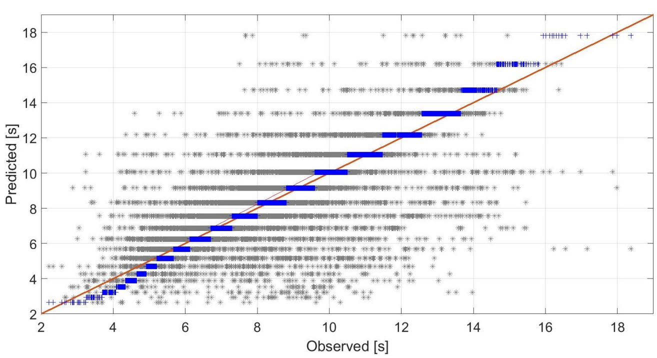

Fig. 5. The period of spectral peak, forecast +24 (SWAN).

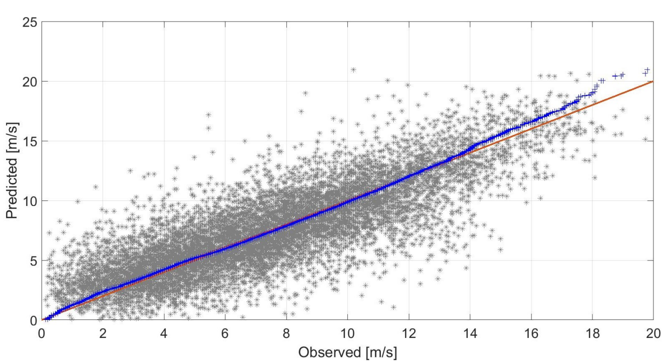

Fig. 6. The wind speed at 10 m height, forecast +24.

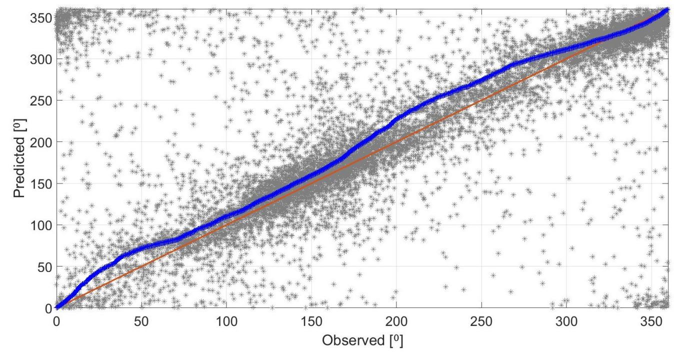

Fig. 7. The wind direction at 10 m height, forecast +24.

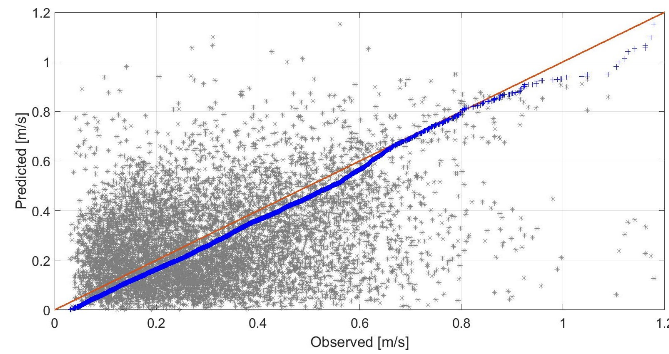

Fig. 8. The current speed at 10 m depth, forecast +24 (POM).

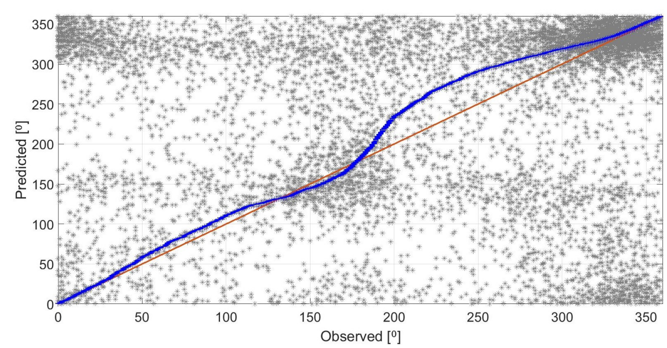

Fig. 9. The current direction at 10 m depth, forecast +24 (POM).

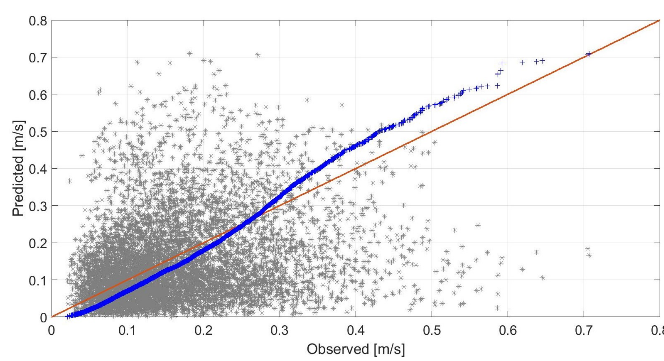

Fig. 10. The current speed at 100 m depth, forecast +24 (POM).

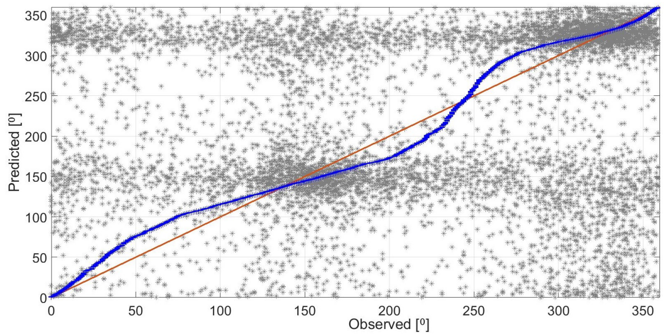

Fig. 11. The current direction at 100 m depth, forecast +24 (POM).

1) The significant wave height: H_{m0} is observed to be higher than 1.5 m, 44% of the time. According to forecast +3 and forecast +24, are H_{m0} >1.5 m, 54% and 53% of the time, respectively. In Table V values of HR and FAR are listed and these values will be discussed in Section VI-C.

TABLE V
THE HIT RATE AND FALSE ALARM RATIO FOR THE SIGNIFICANT WAVE HEIGHT.

	Forecast +3		Forecast +24	
Event	HR	FAR	HR	FAR
$H_{m0} \leq 1.5$ m	0.79	0.05	0.79	0.06
$H_{m0} > 1.5$ m	0.95	0.22	0.94	0.22

2) The period of spectral peak: The minimum observed value of T_p is 2.22 s and the minimum predicted value is T_p=2.66 s. In Table IV the maximum values are presented.

3) The maximum wave height: The measured maximum wave height exceeds 3.5 m 14% of the time.

4) The current at 10 m depth, forecast +24: When the forecast predicts the speed to be between 1-1.2 m/s, the observed speed is <0.8 m/s. When it is observed speed between 1-1.2 m/s, the forecast predicts the speed to be <0.4 m/s, 64% of the times. Both forecast and measurements agree that the flow directions 300°-360° are strongly represented. The $HR_{300^\circ-360^\circ}$=0.70 and the $FAR_{300^\circ-360^\circ}$=0.45.

In 2010, was it three periods with current speed stronger than 1 m/s. The first period was 21.-23. of February. During the night the current flows towards east. With time, the direction is moving clockwise and by noon the 22nd, the current is flowing north, north-west. At the same time, the current speed increases from 0.3 m/s to 1 m/s. When this increase is observed the speed is predicted to be less than 0.1 m/s. During the 12-hour period with strong currents, the direction is changing, but mostly coming from south. Overall, the predicted direction of the current is relatively acceptable, except for in the morning the 22nd. Then it is the opposite of what is observed. Other parameters are relatively constant; the wind comes from south with a speed of 13 m/s, as predicted; the mean significant wave height is 1.6 m, 0.5 m lower than predicted.

Current speed >1.1 m/s was also observed on the 1.-2. of December. Both the forecast and the measurement agree that the current flows towards north trough the entire period. The predicted current speed is significantly lower than the observed, at best the prediction is 30% of the observed value. The other parameters are approximately constant, with easterly wind at 5.5 m/s and a significant wave height of 0.5 m, according to both observations and predictions.

September 27.-28., current was flowing towards north, according to observation and prediction. A maximum speed of 1.1 m/s was observed. The predicted maximum was 0.9 m/s. No measurements of wind and waves were taken at those days.

Twice, current speed above 1 m/s was predicted. In the early morning at 15th of July, the forecast and the observation agree that the wind direction will change from north to south. The forecast predicts current speed around 1 m/s, but current speed, wind speed and significant wave height are estimated to be higher than observed.

October 6., the current flowed towards north, according to observation and prediction. A maximum speed of 0.6 m/s was observed. The predicted maximum was 1.1 m/s. No measurements of wind and waves were taken at those days.

5) The current at 100 m depth, forecast +24: The strongest currents observed are in the region 0.6-0.8 m/s, for all of those cases the forecast predicted the current speed to be below 0.2 m/s. The $HR_{300^\circ-360^\circ}$=0.65 and the $FAR_{300^\circ-360^\circ}$=0.47.

6) The salinity: The weather forecast predicts the salinity to be in the region 30-34 PSU, while the observed salinity covers the region 26-35 PSU.

B. Ocean current data from 2016

The different correlation coefficients are listed in Table VII. Values of standard deviation and mean are listed in Table VIII, with maximum and 99%-quantile values in Table IX. Information about the data recovery rate and the number of comparison points are listed in Table VI.

TABLE VI
THE TOTAL NUMBER OF POINTS COMPARED AND THE LENGTH OF THE COMPARISON PERIOD AND ITS DATA RECOVERY RATE.

Parameter	Length of period	Number of points	Data recovery rate
Surface current	26 days 7 hours	552	100%
Current 100m	26 days 7 hours	552	100%

TABLE VII
THE CORRELATION COEFFICIENTS BETWEEN THE WEATHER FORECAST +3 AND THE MEASURED VALUES.

Parameter	r_{+3}
Surface current speed	0.49
Surface current direction	0.21
Current speed 100 m	0.22
Current direction 100 m	0.13

TABLE VIII
VALUES OF MEAN AND STANDARD DEVIATION, FORECAST +3.

	Mean		Standard deviation	
	Predicted	Observed	Predicted	Observed
CS Surface [m/s]	0.32	0.34	0.18	0.19
CS100m [m/s]	0.17	0.20	0.10	0.10

TABLE IX
VALUES OF 99%-QUANTILE AND MAXIMUM, FORECAST +3.

	99%-quantile		Max	
	Predicted	Observed	Predicted	Observed
CS Surface [m/s]	0.76	0.97	0.81	1.01
CS100m [m/s]	0.43	0.49	0.47	0.63

In Figures 12-15 are the scatter plot grey dots, the q-q plot blue dots and the red line shows the observation equal to the forecast.

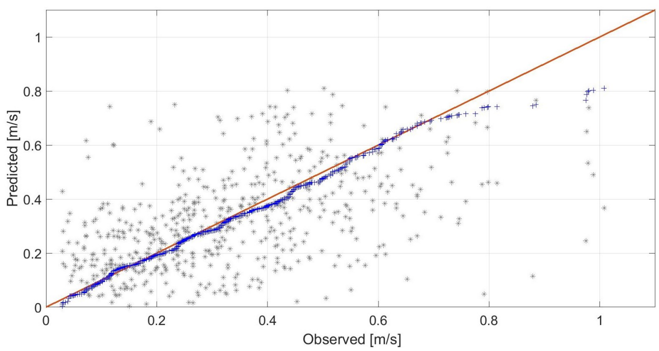

Fig. 12. The surface current speed, forecast +3 (ROMS).

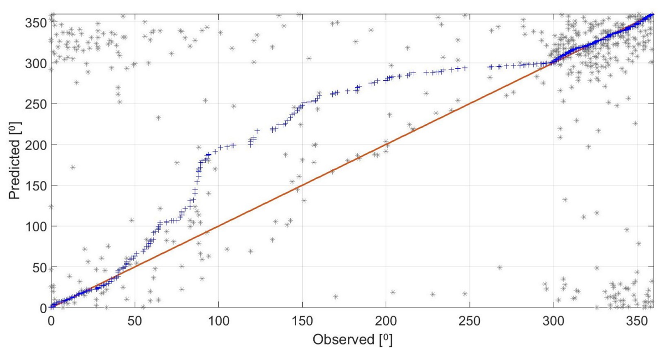

Fig. 13. The surface current direction, forecast +3 (ROMS).

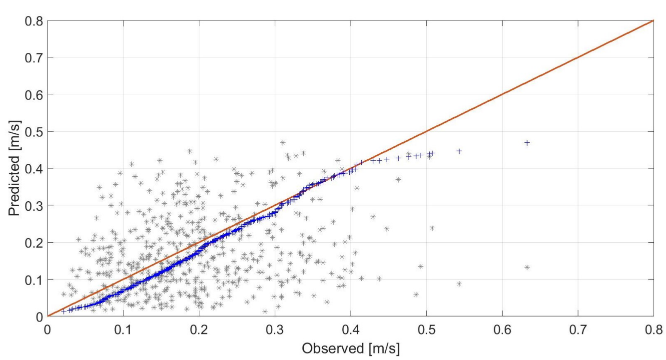

Fig. 14. The current speed at 100 m depth, forecast +3 (ROMS).

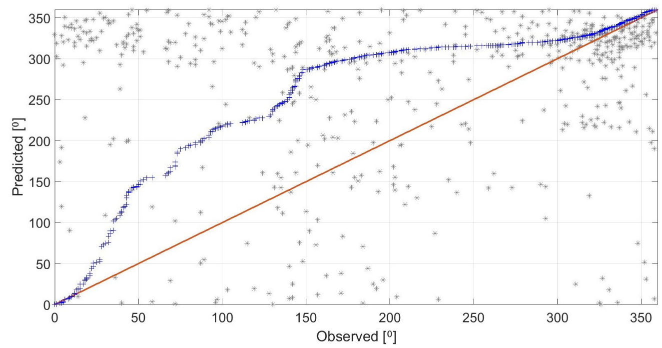

Fig. 15. The current direction at 100 m depth, forecast +3 (ROMS).

1) Surface current: Current speed was measured to be >1 m/s once, and it was not predicted. A few times the speed was predicted to be >0.8 m/s, then it was observed to be between 0.4-0.8 m/s. The $HR_{300^\circ-360^\circ}$=0.67 and the $FAR_{300^\circ-360^\circ}$=0.33.

2) Current at 100m depth: At this depth, the $HR_{300^\circ-360^\circ}$=0.72 and the $FAR_{300^\circ-360^\circ}$=0.55.

C. The current of both ocean models

The hit rate and false alarm ratio of different events are presented in Table X and XI. The forecast +3 to +24 have been used.

TABLE X
THE HIT RATE AND FALSE ALARM RATIO FOR POM AT 10 M DEPTH AND ROMS AT THE SURFACE, FORECAST +3.

	POM		ROMS	
Event	HR	FAR	HR	FAR
CS $\leq$ 0.2 m/s	0.49	0.61	0.55	0.49
CS $\leq$ 0.4 m/s	0.85	0.22	0.84	0.22
CS $\leq$ 0.6 m/s	0.96	0.06	0.93	0.08
CS >0.6 m/s	0.29	0.66	0.29	0.70
CS >0.8 m/s	0.33	0.67	0	1
CS >1.0 m/s	0	1	0	NaN

TABLE XI
THE HIT RATE AND FALSE ALARM RATIO FOR ROMS AND POM, AT 100 M DEPTH, FORECAST +3.

	POM		ROMS	
Event	HR	FAR	HR	FAR
CS $\leq$ 0.2 m/s	0.81	0.24	0.71	0.36
CS $\leq$ 0.4 m/s	0.95	0.02	0.98	0.03
CS $\leq$ 0.6 m/s	1.00	0.00	1	0.00
CS >0.6 m/s	0	1	0	NaN
CS >0.4 m/s	0.14	0.93	0.12	0.85

VI. DISCUSSION

A. Sources of error

The buoy measurements of waves are based on the wave spectrum of 10 or 20 minute of data, which will show more variability than the hourly model output by SWAN [30]. This causes a difference between the forecast and the measurements, which can not be blamed bad weather forecast.

The Seawatch buoy defines swell and wind sea by different frequencies, this is a simplification, which affects the result [31].

For wind and currents, the forecast are relative to the mean sea level, while the measurements are relative to the buoys movement. In rough weather, the sensors will be tilted. These facts affects the results.

The wind measurements at 3.5 m are influenced by the waves, as 14% of the waves are higher than 3.5 m. The measured wind has been extrapolated and the wind direction is measured at 3.5 m while estimated at 10 m. These are also sources of error.

In Table II it can be seen that the salinity has low values of r. Among other factors, this is a result of the observed region being broader than the predicted, see Section V-A6. The changes in the salinity affects the current flow, therefore an improved prediction of the salinity will improve the forecast of the current. The pressure is also important for the modelling of the current. As the pressure has r=1.00, this is not the reason for the bad predictions of the current.

The precision of the forecast +3 are different from for example the forecast +7. This has not been taken into account. However, neither do the forecast given to the users. The accuracy in the sensors are not major, see Section III.

It can be doubted if one month of data is enough to verify a model, but it gives an indication. The one month of data from 2016 might contain some noise, truly caused by tilt of the sensor [32]. The data from 2009-2011 were more processed to get read of incorrect measurements.

B. Wind at 10 m

The q-q plot of the wind speed in Figure 6 follows a relatively straight line equal to the red line. This implies that the marginal distribution of the weather forecast and the marginal distribution of the observed wind speed are similar. This is verified by the values of mean and standard deviation in Table III. When the predicted wind speed is 15 m/s or higher, the observed speed tends to be lower. This can be seen from the scatter plot and starts where the q-q plot exceeds the red line in Figure 6. As strong wind are connected to high waves, it is reasonable to believe that those wind measurements are affected by the waves. From this, one would expect the 99.9%-quantile and maximum values of the forecast to be higher than what is observed. In Table IV, this is confirmed, and the values are 7% and 6% higher, respectively. If the measurements were not affected by the sea elevation, it is reasonable to assume that the r would be higher.

The scatter plot in Figure 7 shows that sometimes the predicted direction might be opposite from what is observed, but most of the times the weather forecast is relatively good, as the scatter plot has a high density around the red line. Wind might change direction relatively fast, such as a minor time delay in the forecast will effect the correlation significantly. Both the forecast and the measurement tell that most of the wind comes from south/south-east (120°-200°) or north-west (300°-360°). Since 360° and 0° are the same point the data correlate slightly better than the calculated r_{+24}=0.70.

C. The significant wave height

The q-q plot in Figure 3 is a comparatively straight line. This indicates that the marginal distribution of the forecast can be described by the same distribution group as the predicted data. But as the slope of the q-q plot is higher than the the slope of the red line, the marginal distribution of the forecast has a higher mean value than the predictions. In Table III this is confirmed, the predicted mean is 17% higher than the observed. This is in line with the scatter plot, which mostly is positioned above the red line. This tells that the forecast predicts the waves to be higher than what is actually observed, most of the time. The difference between the maximum and the 99.9%-quantile is relatively high for both the predicted and the observed values, 23% and 28% respectively. This indicates that the maximum values are rather rare events.

It is unreasonable that the weather forecast shall be perfect and the obtained r_{+24}=0.92 is respectable. However, one have to have in mind that the linear correlation coefficient is calculated relative to a regression line positioned approximately around the q-q plot. Therefore the r relative to the red line will be slightly lower. The measurements of waves are not effected negatively by the buoys movement and the resolution of the wave model is higher than for wind and current. This can be reason for the forecast of waves being better than the rest.

That the forecast overpredicts H_{m0} minimizes the risk of experiencing higher waves than expected, but it also reduces the number of days an offshore operation can take place. According to Statoils regulations, 1.5 m is the upper limit of H_{m0} accepted to do services on Hywind Demo from a ship. Thus a lower $\mathrm{FAR}_{H_{m0}>1.5m}$ would be preferable, in addition to a higher $\mathrm{HR}_{H_{m0}\leq 1.5m}$, see Table V.

Any significant difference between forecast +3 and forecast +24 can not be found, according to Table III, IV and V. However, the 99.9%-quantile for forecast +3 is 9% higher than the one for forecast +24. This means that the forecast +3 predicts a higher amount of high waves.

D. The significant wave height of swells

The values of mean, maximum, standard deviation and 99.9%-quantiles in Table III and IV do not differ significantly, compared to H_{m0}. Hence, the marginal distribution of the forecast is relatively similar to the observed marginal distribution. This is verified by the q-q plot being located approximately along the red line in Figure 4. The tendency of the forecast to predict higher waves than observed can be seen in this figure as well, but not as significant. This may indicates that the overestimation is strongest for wind waves.

E. The period of spectral peak

The values in Table III and IV tells that the observed marginal distribution is relatively similar to the predicted one. The maximum value is observed to be higher than the predicted. And the minimum value is observed to be lower than the predicted, see Section V-A2. From Figure 5 it can be seen that the resolution of the forecast differ from the buoy measurements. These factors will affect the correlation coefficient negatively, and it is one of the reasons for the lower values of r for T_p than for the wave heights, see Table II.

F. The current at 10 m depth (POM) and the surface current (ROMS)

Ocean model POM. The wide scatter plot in Figure 8 results in r_{+24}=0.34 and tells that the forecast has to be significantly improved. The corresponding q-q plot, and the mean, standard deviation and maximum values in Table III and IV shows that the marginal distributions are relatively similar. However, the q-q plot separates from the red line around 0.9 m/s, which tells that the forecast fails for speeds higher than that. This is also indicated by the difference between the 99.9%-quantile values. The observed value is 11% higher than the predicted, and it tells that strong currents are observed more frequently than predicted. From the three observed times with strong currents, it is hard to find a pattern, see Section V-A4. Though, the current flows north every time, which corresponds with the main direction of the Norwegian coastal current [5]. Two of those times the wind was measured and it was blowing north and west. Looking at the dispersed scatter plot in Figure 9, the q-q plot is surprisingly straight. This means that the time dependent forecast is undependable, while the overall distribution of the forecast gives a fair indication of what to expect at the site.

Ocean model ROMS. According to values of mean and standard deviation in Table VIII, the marginal distributions of forecast and prediction are similar. By looking at the q-q plot in Figure 12 it can be seen that this is true for current speeds below 0.7 m/s. The similarity between observations and predictions diminishes for higher values, observed maximum speed is 27% higher than the predicted, see Table IX. The direction is mostly towards north-west according to both predictions and measurements. The q-q plot in Figure 13 tells that the forecast deviate from the observations for directions between 50°-300°, meaning that these directions are observed more frequently than predicted.

G. The current at 100 m depth

Ocean model POM. The scatter plot in Figure 10 indicates that when strong currents are predicted, low values are observed and the other way around. The predicted and observed maximum values are equal, while the forecast predicts a higher amount of strong currents according to the 99.9%-quantile value being higher, see Table IV. The mean and standard deviation values in Table III indicate that the marginal distributions are similar. The q-q plot is positioned above the red line for speeds >0.3 m/s. This tells that the predicted marginal distribution has a higher frequency of current speeds above 0.3 m/s, relative to the observed marginal distribution. Figure 11 shows that the forecast predicts the current to flow towards north-west (300°-360°) or towards south-east (120°-170°), most of the time. The observations agree that those directions are frequently present, but a wider variation in the flow directions are observed.

Ocean model ROMS. ROMS predicts a high amount of the current to flow towards north, north-west, which is also observed to be the main direction. But a wider distribution of flow directions are observed, see Figure 15. The q-q plot in Figure 14, approximately follows the red line up to 0.4 m/s. The difference in maximum values are significant according to Table IX, and the strongest currents are not predicted.

H. Concluding remarks on the two ocean models POM and ROMS

According to the values in Table II-IV, forecast +3 and forecast +24 are approximately similar. Exceptions are that values of maximum and 99.9%-quantile are lower for forecast +3 than forecast +24, at 10 m depth. However, it is acceptable to compare the forecast +24 of POM, with the forecast +3 of ROMS.

Table IV shows that the maximum values are approximately equal for predictions of POM and observations. The maximum values predicted by ROMS are significantly lower than what are observed, see Table IX. According to Table X and XI, are values of HR and FAR quite similar for both models. High values of FAR for speeds >0.6 m/s, are present for both models. Therefore it can not be concluded that POM is better than ROMS to predict strong currents. This is confirmed in Section V-A4, were it was emphasized that predicted strong currents are not related to observed strong currents. More data about strong currents, of both forecast and observations, would be desirable to characterize the behaviour of ROMS.

The q-q plots in Figure 9 and 11 of POM and in Figure 13 and 15 of ROMS, do not have the same shapes. This is a result of ROMS not predicting as much flow around 180° as POM. This might be good as it agrees more with the observations. However, the values of $HR_{300^\circ-360^\circ}$ and $FAR_{300^\circ-360^\circ}$ do not show any improvements from POM to ROMS, see Section V-A4 and V-A5, and Section V-B1 and V-B2.

In Section III-C the complexity of the ocean current was emphasized. It shows that the knowledge of the ocean is broad. However, to model all phenomena well, buoy measurements from several areas are needed to give good initial conditions. It is a minimal amount of ongoing measurements of the ocean, which decreases the quality of the current forecast [30]. Both ROMS and POM are known to be best for tide and wind driven currents [30], which does not match with the main driving forces of the current at the Hywind Demo site. An upside of the models, are their applicability to detecting rescue objects and oil spill [33].

VII. CONCLUSION

The comparison of the weather forecast one day ahead with the measured data at the Hywind Demo site, have given following results. The linear correlation coefficients for the wind speed at 10 m height and the significant wave height, are 0.82 and 0.92, respectively. Hence, the forecast of both wind and waves are relatively good.

Any noticeable difference between the ocean models POM and ROMS can not be found. Both struggles with estimating strong currents and in general the forecast can not be trusted. Only 30% of the observed times, did the forecast predict the surface current to be stronger than 0.6 m/s. This is true for both models.

If it is of interest to know the characteristics of a site, the weather forecast from one year can be used. As it seems to give a reasonable estimate of which loads an object will experience. Exceptions are that stronger surface currents will most likely occur and lower waves are to be expected.

Further work

- Compare more data of ROMS, to obtain a better assessment.
- Characterize which weather conditions the forecast predicts satisfactory and which not.
- Investigate long-term forecast in order to outline its reliability.
- Locate an area that is well documented by buoys, implement their measurements to the ocean models and verify their results.

Acknowledgement

The author would like to thank Statoil, Fugro OCEANOR and MET Norway by Birgitte Furevik for acquisition of data and general information. Thanks to NTNU by Lars Sætran, for guidance and an educational year.

References

[1] Statoil. (2014) Hywind demo. [Online]. Available: http://www.statoil.com/no/TechnologyInnovation/NewEnergy/RenewablePowerProduction/Offshore/Hywind/Pages/HywindPuttingWindPowerToTheTest.aspx

[2] Meteorologisk institutt. [Online]. Available: http://www.met.no/

[3] A. E. Onstad, M. Stokke, and L. Sætran, "Site Assessment of the floating wind turbine Hywind Demo," *Energy Procedia*, 2016, under review.

[4] K. Torsethaugen, *Simplified double peak spectral model for ocean waves*. Trondheim: SINTEF, Fisheries and Aquaculture, 2004.

[5] R. Sætre, Ed., *The Norwegian Coastal Current - Oceanography and Climate*. Tapir Academic Press, 2007.

[6] J. A. Johannessen, R. A. Shuchman, G. Digranes, D. R. Lyzenga, C. Wackerman, O. M. Johannessen, and P. W. Vachon, "Coastal ocean fronts and eddies imaged with ERS 1 synthetic aperture radar," *Journal of Geophysical Research*, vol. 101, no. C3, pp. 6651–6667, 1996.

[7] ECMWF. Forty years of advancing global nwp through co-operation. [Online]. Available: http://www.ecmwf.int/

[8] G. L. Mellor, "Users guide for a three-dimensional, primitive equation, numerical ocean model," Princeton University, 2002.

[9] IMCS, Ocean Modeling Group. Regional Ocean Modeling System (ROMS). [Online]. Available: http://myroms.org/

[10] Fugro OCEANOR. (2016) Seawatch buoy. [Online]. Available: http://www.oceanor.no/seawatch/buoys-and-sensor/Seawatch

[11] T. R. Instruments. (2009) Workhorse sentinel. [Online]. Available: http://rdinstruments.com/__documents/Brochures/sentinel_datasheet_lr.pdf

[12] N. AS. Aquadopp profile brochure. [Online]. Available: http://www.nortek-as.com/lib/brochures/aquadopp-profiler/view

[13] K. S. AS. Seatex mru 4 the orientation and heave sensor. [Online]. Available: http://www.escort.com.pl/images/escort/pdf/hydrografia/Kongsberg_MRU_4_ang.pdf

[14] Y. Company. (2007) Model 85106 ultrasonic anemometer. [Online]. Available: http://www.youngusa.com/Brochures/85106(1007).pdf

[15] DNV-RP-C205, *Environmental conditions and environmental loads*. Det Norske Veritas, April 2007.

[16] S. A. Hsu, E. A. Meindl, and D. B. Gilhousen, "Determining the power-law wind-profile exponent under near-neutral stability conditions at sea," *Journal of Applied Meteorology 33*, 1993.

[17] D. Myrhaug, "Kompendium TMR 4180 Marin dynamikk - Uregelmessig sjø," Institutt for marin teknikk, NTNU, 2007.

[18] I. R. Young, *Wind Generated Ocean Waves*. Elsevier Ocean Engineering Book Series, 1999, vol. 2.

[19] Einar Nygaard, personal communication, Statoil ASA, 2016.

[20] R. H. Stewart, *Introduction To Physical Oceanography*. Texas, United States: Department of Oceanography, Texas A&M University, September 2008.

[21] Universitetet i Oslo. Almanakk-komiteen., *Almanakk for Norge 2010 for året etter Kristi fdsel*. Gyldendal, 2009.

[22] E. Brown, A. Colling, D. Park, J. Phillips, D. Rothery, and J. Wright, *Seawater: Its composition, properties and behaviour*. The Open University, 1997.

[23] A. J. Wheeler and A. R. Ganji, *Introduction to Engineering Experimentation*, 3rd ed. PEARSON, 2010.

[24] R. E. Walpole, R. H. Myers, S. L. Myers, and K. Ye, *Probability & Statistics for Engineers & Scientists*. Pearson Prentice Hall, 2007.

[25] E. Kreyszig, *Advanced Engineering Mathematics*, 9th ed. John Wiley & Sons, 2006.

[26] M. Homleid and F. T. Tveter, "Verification of operational weather prediction models september to november 2015," *Meteorology*, no. 16, 2016.

[27] P. Berens, "CircStat: A MATLAB Toolbox for Circular Statistics," *Journal of Statistical Software*, vol. 31, no. 1, 2009.

[28] S. R. Jammalamadaka and A. S. Gupta, *Topics in circular statistics*. World Scientific, 2001.

[29] N. I. Fisher, *Statistical Analysis of Circular Data*. Cambridge University Press, 1993.

[30] Birgitte Rugaard Furevik, personal communication, Norwegian Meteorological Institute, 2016.

[31] L. Z.-H. Chuang, L.-C. Wu, and J.-H. Wang, "Continuous wavelet transform analysis of acceleration signals measured from a wave buoy," *Sensors*, vol. 13, 2013.

[32] Lasse Lønseth, personal communication, Fugro OCEANOR AS, 2016.

[33] Ø. Breivik and A. A. Allen, "An operational search and rescue model for the norwegian sea and the north sea," *Journal of Marine Systems*, vol. 69, 2007.